

# Control of Three Phase 7-Level CHB Voltage-Source Active Rectifier

Vojtech Blahnik, Jakub Talla, Tomas Kosan, Zdenek Peroutka

Regional Innovation Centre for Electrical Engineering

University of West Bohemia

Pilsen, Czech Republic

lucke@rice.zcu.cz, talic@rice.zcu.cz, kosan@rice.zcu.cz, peroutka@ieee.org,

**Abstract –** This paper introduces control algorithm of three-phase seven level cascaded H-bridge operates as voltage source active rectifier. The proposed control strategy combines PI and PR controllers with mathematical model of converter current loop and provide direct current control with voltage balancing. The theoretical conclusions are verified by simulations made for small-scale laboratory prototype.

**Keywords-multilevel converter; active rectifier; current control; voltage balancing**

## I. INTRODUCTION

This project has been made in cooperation with our industrial partner and the main objective of this research has been the analysis and design of control algorithm for three-phase seven level cascaded H-bridge (CHB) voltage-source active rectifier, connected directly to ac grid without transformer. This multilevel voltage-source active rectifier (VSAR), connected directly to 6kV ac-grid must provide: (i) the sum of dc-link voltage in each phase is equal to demanded value ( $U_{cw}$ ), (ii) the distribution of dc-link voltage on each power cell is identical to demanded value ( $U_{c\_mXw} = U_{cw}/3$ ), and (iii) Low current ripple and sinusoidal waveform. These three requirements must be ensured by selecting suitable control algorithm.

The solution presented in this contribution is based on CHB converter – this configuration is well-known for medium-voltage CHB converters, e.g. [1]-[11], where it is used as a solution for PV systems connected directly to the power grid, static compensators and active filters, medium-voltage converters for EV charging stations.

The popular modulation technique is in this case phase shifted PWM (PS-PWM), which is well described in many publications, see e.g. [2], [3] and [12]- [14]. The designed converter topology include proposed control algorithm was tested on simulation model for low-voltage converter prototype power circuit diagram shown in Figure 1.

## II. CONVERTER CONTROL

Proposed control strategy of CHB VSAR uses three separate control loops (these control loops are the same and each is intended for single phase – a, b, c). These control loops uses PI controller for sum dc-links voltage control ( $R_{Uc}$ ), PR controller for direct

control of the fundamental harmonic of ac current ( $R_i$ ) and extra voltage balancing PI controllers ( $R_{\Delta U_{c\_m2}}$  and  $R_{\Delta U_{c\_m3}}$ ). The designed control configuration of CHB VSAR is depicted in Figure 2. It is standard control strategy providing direct current control for single-phase system (presented e.g. in [15] and [16]) and voltage balancing at individual power cells is adjusted by PI controllers  $R_{\Delta U_{c\_m2}}$  and  $R_{\Delta U_{c\_m3}}$ . These controllers only modify the value of modulation signals (duty cycle)  $u_{v\_m2}$   $u_{v\_m3}$ . Therefore, the voltage balancing is in master mode for first cell ( $U_{c\_m1}$ ) and slave modes for second cell ( $U_{c\_m2}$ ) and third cell ( $U_{c\_m3}$ ).

The control strategy for the phase\_a is shown in Figure 2. The PI controller ( $R_{Uc\_a}$ ) is used for control sum of dc-link voltage ( $\Delta U_{c\_a}$ ) to required value  $U_{cw}$ . This value ( $\Delta U_{c\_a}$ ) is sum of voltage on separated dc-links of phase\_a. It is evident from (1). The output signal of controller  $R_{Uc\_a}$  is magnitude ( $I_m$ ) of required current for phase\_a. From magnitude  $I_m$  and ac source voltage position ( $\vartheta_a$ ) is calculated value of required current  $i_{wa}$ , (2). The input value for current controller  $R_{ia}$  (proportional resonant controller ...PR type) is control error  $e_{i\_a}$  and it is difference between actual current  $i_a$  and required current  $i_{wa}$ . The output signal of controller  $R_{ia}$  is correction part  $u_{v\_PR\_a}$  and this part is summed with the estimate signal  $u_{v\_estim\_a}$ . The resulting value  $u_{v\_m1\_a}$  enters into PWM modulator and by firing pulses is switched the first cell (1xHb) of phase\_a. Computation of the estimated signal  $u_{v\_estim\_a}$  is based on a simplified model of VSAR and it is necessary to know the magnitude ( $U_m$ ) and position ( $\vartheta_a$ ) of the ac source voltage ( $u_a$ ), as shown in the (3). The second and the third cell (1xHb) of phase\_a is switched by PWM modulator (in this case PS-PWM with shifted carriers) by using control signals  $u_{v\_m2\_a}$  and  $u_{v\_m3\_a}$ . The value of these modulation signals (duty cycles) are adjusted with respect to balancing of dc-links cell for the phase\_a. As a balancing controllers are used PI controllers  $R_{\Delta U_{c\_m2}}$  and  $R_{\Delta U_{c\_m3}}$ , these controllers only modify the value of modulation signals (duty cycles)  $u_{v\_m2\_a}$ ,  $u_{v\_m3\_a}$  against the main signal  $u_{v\_m1\_a}$  as a shown in Figure 2. The correction output signals ( $\Delta u_{v\_m2\_a}$ ,  $\Delta u_{v\_m3\_a}$ ) are multiplied by the sign of requirement current magnitude ( $\text{sign}(I_m)$ ). The main modulation signals (duty cycles)  $u_{v\_m2\_a}$  is calculated from the phase current  $i_a$  and sum of dc-links voltage  $\sum U_{c\_a}$ . The PS-PWM with shifted carriers is used for the modulation of converter. The major benefit of employed shifted carriers is the

significant decrease of the ac current ripple due to multilevel nature of the voltage at the converter ac terminals. In our particular case with three modules in series, the phase-voltage at the converter ac side is seven-level (Illustration of modulation and saw signal with resulting phase voltage at the converter ac terminals is depicted in Figure 3. The number of voltage levels for CHB converter is given by (4). The shifted carriers and resulting reduced ac current ripple have positive impact on the converter input inductance design (There is less transitions between voltage levels – 7 levels).

$$\sum U_{c,a} = U_{c,m1,a} + U_{c,m2,a} + U_{c,m3,a} \quad (1)$$

$$i_{wa} = I_m \cdot \sin(\vartheta_a) \quad (2)$$

$$u_{v,estim,a} = U_m \cdot \sin(\vartheta_a) \quad (3)$$

$$V_{levels} = 2 \cdot N + 1 \quad (4)$$

### III. CONVERTER SIMULATION RESULTS

The proposed control of VSAR was tested on simulation model of three-phase CHB converter. This simulation model is composed of three-phase voltage sources ( $u_a$ ,  $u_b$ ,  $u_c$ ), input inductance  $L$ , three H-bridge for each phase connected in series. The converter load is simulated by nine individual current sources ( $i_{z,a,M1}$  -  $i_{z,c,M3}$ ). The simulation model of the CHB VSAR has been designed in language C. For the calculation of differential equations we use Euler difference formula of the first order, the simulation step size is of  $0.1\mu s$ . In this simulation we have tested discrete control algorithm which is depicted in Figure 2. The sampling period of controllers was  $50\mu s$ , this short sampling period of control was chosen as to obtain precisely summation at the control algorithm (especially for calculation of resonant controllers).

The Figure 4. shows simulation result of the CHB active rectifier under steady-state condition. The waveforms  $i_a$ ,  $i_b$ ,  $i_c$  represents ac phase currents which are harmonic and in phase with ac-grid voltage  $u_a$ ,  $u_b$ ,  $u_c$ . The output dc-link voltage at individual power cells for step change of load from 0 kW to 9.45 kW is shown in Figure 5. In this case the symmetrical load was simulated by nine equivalent current sources ( $i_{z,a,M1}=7A$ ,  $i_{z,a,M2}=7A$ ,  $i_{z,a,M3}=7A$ ,  $i_{z,b,M1}=7A$ ,  $i_{z,b,M2}=7A$ ,  $i_{z,b,M3}=7A$ ,  $i_{z,c,M1}=7A$ ,  $i_{z,c,M2}=7A$ ,  $i_{z,c,M3}=7A$ ). The ripple of controlled dc-link voltages (at each of individual power cell) has the dominant frequency of double grid voltage frequency. This distortion is coming-out from physical properties of single-phase voltage-source active rectifier type of converter. The Figure 6. shows the response of CHB active rectifier to step change of non-symmetrical load ( $i_{z,a,M1}=7A$ ,  $i_{z,a,M2}=7.3A$ ,  $i_{z,a,M3}=7.6A$ ,  $i_{z,b,M1}=5.6A$ ,  $i_{z,b,M2}=5A$ ,  $i_{z,b,M3}=5.3A$ ,  $i_{z,c,M1}=5A$ ,  $i_{z,c,M2}=6A$ ,  $i_{z,c,M3}=7A$ ). The simulation result shows satisfactory operation of the balancing controllers. In this case the non-symmetrical load is reflected in the differences at ac currents value and by the current ripple differences as shown in Figure 7.

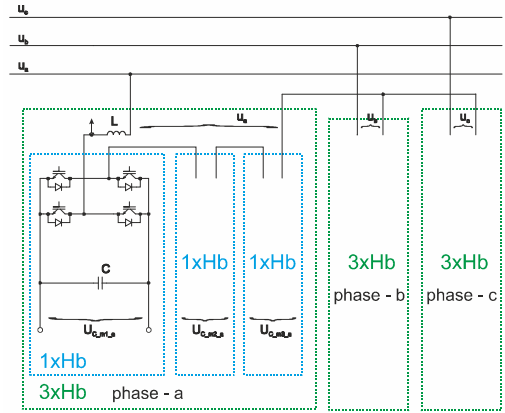


Figure 1. Configuration of designed three phase 7-Level CHB Voltage-Source Active Rectifier

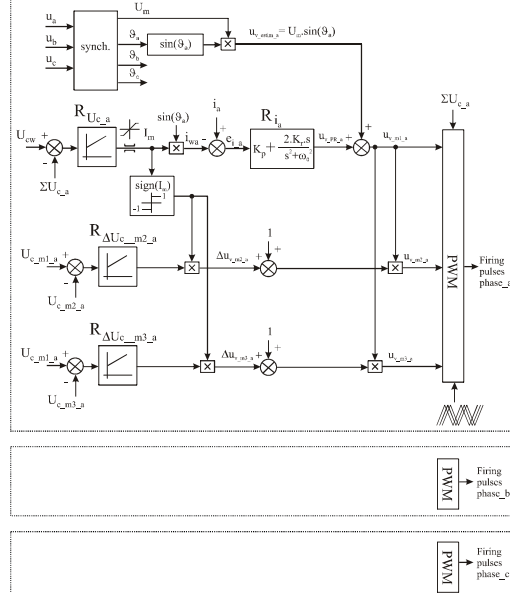


Figure 2. Proposed control of three phase 7-Level CHB Voltage-Source Active Rectifier

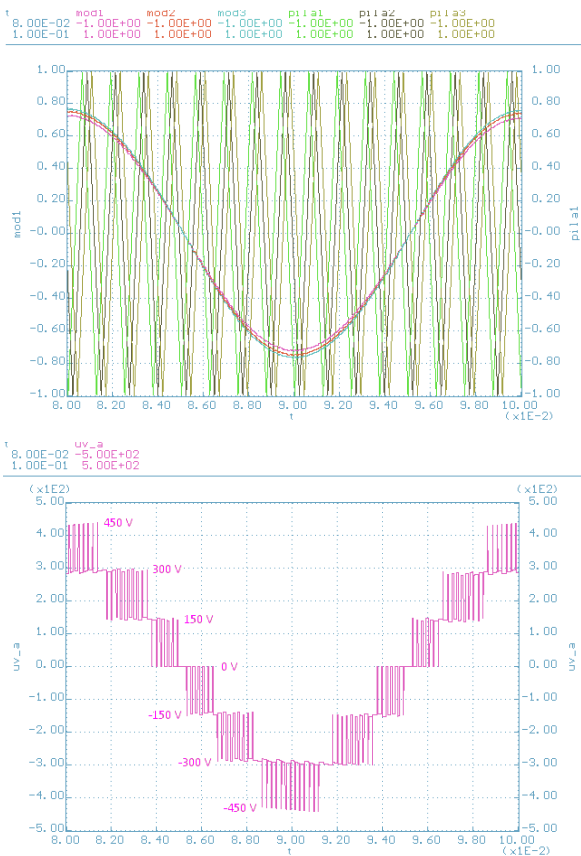


Figure 3. modulation and saw signals with resulting ac voltage phase for single-phase

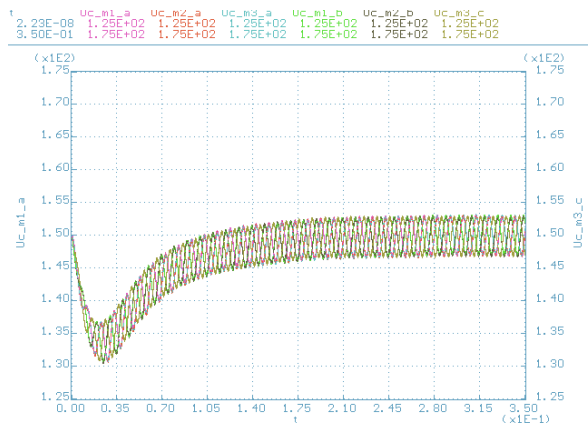


Figure 5. Behaviour of dc-link voltages on selected cells for step change of load ( $P = 0 \text{ kW} \rightarrow 9.45 \text{ kW}$  during symmetrical load).

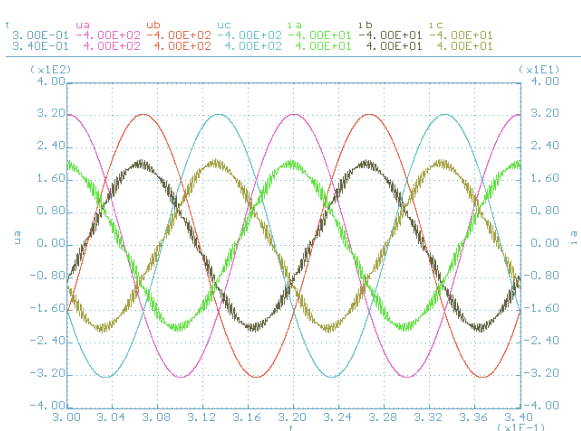


Figure 4. Voltages and currents of VSAR under steady-state conditions in rectifier mode (symmetrical load  $P = 9.45 \text{ kW}$ )

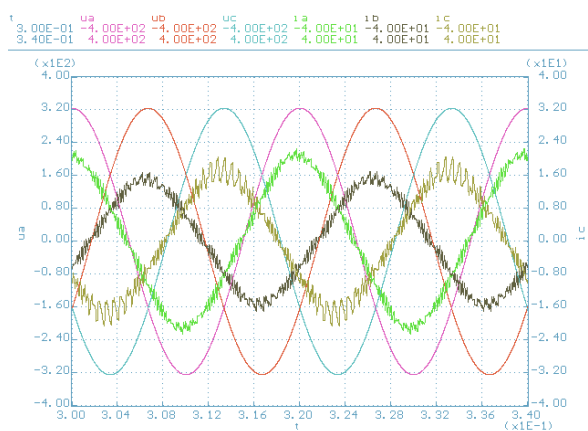


Figure 6. Behaviour of dc-links voltage on selected cells for step change of load (non-symmetrical load).

Figure 7. Phase-voltages and currents of VSAR under steady-state conditions in rectifier mode (during non-symmetrical load).

#### IV. CONSLUSIONS

This paper present control designed for cascaded H-bridge voltage-source active rectifier with harmonic current waveform. This control provides a sufficiently fast control of the output dc voltage for step change of the load. Proposed control enables active voltage balancing for each of individual power cells under non-symmetrical converter load (tested for 33% non-symmetrical load of phase c). The control provides voltage balancing on individual power cells directly at the control structure level. This is the simple and powerful approach which can be easily implemented using conventional PR and PI controllers which are industry-standard components. The remaining problems are slow dynamics of balancing one second in this case and voltage balancing during zero load of active rectifier.

#### ACKNOWLEDGMENT

This research has been supported by the European Regional Development Fund and the Ministry of Education, Youth and Sports of the Czech Republic under project No. CZ.1.05/2.1.00/03.0094: Regional Innovation Centre for Electrical Engineering (RICE) and project No. SGS-2015-038.

#### REFERENCES

- [1] Cortes, P.; Wilson, A.; Kouro, S.; Rodriguez, J.; Abu-Rub, H., "Model Predictive Control of Multilevel Cascaded H-Bridge Inverters," *Industrial Electronics, IEEE Transactions on*, vol.57, no.8, pp.2691,2699, Aug. 2010
- [2] Watson, A.J.; Wheeler, P.W.; Clare, J.C., "A Complete Harmonic Elimination Approach to DC Link Voltage Balancing for a Cascaded Multilevel Rectifier," *Industrial Electronics, IEEE Transactions on*, vol.54, no.6, pp.2946,2953, Dec. 2007
- [3] Vazquez, S.; Leon, J.I.; Carrasco, J.M.; Franquelo, L.G.; Galvan, E.; Reyes, M.; Sanchez, J.A.; Dominguez, E., "Analysis of the Power Balance in the Cells of a Multilevel Cascaded H-Bridge Converter," *Industrial Electronics, IEEE Transactions on*, vol.57, no.7, pp.2287,2296, July 2010
- [4] Rivera, S.; Kouro, S.; Wu, B.; Leon, J.I.; Rodriguez, J.; Franquelo, L.G., "Cascaded H-bridge multilevel converter multistring topology for large scale photovoltaic systems," *Industrial Electronics (ISIE), 2011 IEEE International Symposium on*, vol., no., pp.1837,1844, 27-30 June 2011
- [5] Kouro, S.; Fuentes, C.; Perez, M.; Rodriguez, J., "Single DC-link cascaded H-bridge multilevel multistring photovoltaic energy conversion system with inherent balanced operation," *IECON 2012 - 38th Annual Conference on IEEE Industrial Electronics Society*, vol., no., pp.4998,5005, 25-28 Oct. 2012
- [6] Rivera, S.; Bin Wu; Kouro, S.; Hong Wang; Donglai Zhang, "Cascaded H-bridge multilevel converter topology and three-phase balance control for large scale photovoltaic systems," *Power Electronics for Distributed Generation Systems (PEDG), 2012 3rd IEEE International Symposium on*, vol., no., pp.690,697, 25-28 June 2012
- [7] Townsend, C.D.; Summers, T.J.; Betz, R.E., "Control and modulation scheme for a Cascaded H-Bridge multi-level converter in large scale photovoltaic systems," *Energy Conversion Congress and Exposition (ECCE), 2012 IEEE*, vol., no., pp.3707,3714, 15-20 Sept. 2012
- [8] Cortes, P.; Kouro, S.; Barrios, F.; Rodriguez, J., "Predictive control of a single-phase cascaded h-bridge photovoltaic energy conversion system," *Power Electronics and Motion Control Conference (IPEMC), 2012 7th International*, vol.2, no., pp.1423,1428, 2-5 June 2012
- [9] Aleenejad, M.; Iman-Eini, H.; Farhangi, S., "Modified space vector modulation for fault-tolerant operation of multilevel cascaded H-bridge inverters," *Power Electronics, IET*, vol.6, no.4, pp.742,751, April 2013
- [10] Vasiladiotis, M.; Rufer, A., "A Modular Multiport Power Electronic Transformer With Integrated Split Battery Energy Storage for Versatile Ultrafast EV Charging Stations," *Industrial Electronics, IEEE Transactions on*, vol.62, no.5, pp.3213,3222, May 2015
- [11] Rojas, C.A.; Kouro, S.; Edwards, D.; Bin Wu; Rivera, S., "Five-level H-bridge NPC central photovoltaic inverter with open-end winding grid connection," *Industrial Electronics Society, IECON 2014 - 40th Annual Conference of the IEEE*, vol., no., pp.4622,4627, Oct. 29 2014-Nov. 1 2014
- [12] Darus, R.; Konstantinou, G.; Pou, J.; Ceballos, S.; Agelidis, V.G., "Comparison of phase-shifted and level-shifted PWM in the modular multilevel converter," *Power Electronics Conference (IPEC-Hiroshima 2014 - ECCE-ASIA), 2014 International*, vol., no., pp.3764,3770, 18-21 May 2014
- [13] Ghias, A.M.Y.M.; Pou, J.; Ciobotaru, M.; Agelidis, V.G., "Voltage balancing method for the multilevel flying capacitor converter using phase-shifted PWM," *Power and Energy (PECon), 2012 IEEE International Conference on*, vol., no., pp.274,279, 2-5 Dec. 2012
- [14] Efika, I.B.; Nwobu, C.J.; Zhang, L., "Reactive power compensation by modular multilevel flying capacitor converter-based STATCOM using PS-PWM," *Power Electronics, Machines and Drives (PEMD 2014), 7th IET International Conference on*, vol., no., pp.1,6, 8-10 April 2014
- [15] Blahnik, V.; Peroutka, Z.; Talla, J.; Matuljak, I., "Controlled single-phase current source with LCL filter," *ELEKTRO, 2014*, vol., no., pp.134,137, 19-20 May 2014
- [16] Blahnik, V.; Peroutka, Z.; Talla, J.; Matuljak, I., "Low ripple current source based on resonant controllers," *Industrial Electronics Society, IECON 2013 - 39th Annual Conference of the IEEE*, vol., no., pp.967,972, 10-13 Nov. 2013